Pergamon

PII: S0148-9062(96)00049-6

Int. J. Rock Mech. Min. Sci. Vol. 34, No. 1, pp. 17–25, 1997

0148-9062/97 $17.00 + 0.00

Test Parameter Analysis in Abrasive Water Jet Cutting of Rocklike Materials

A. W. MOMBER†
R. KOVACEVIC‡

This paper contains investigations on the behavior of five artificial rocklike materials subjected to abrasive water jet cutting. The influence of the test parameters, i.e. applied pump pressure, traverse rate and abrasive mass flow rate was investigated, as well as the influence of several material parameters, e.g. compressive strength, Young's modulus, absorbed fracture energy and crack velocity. For the test parameters, it is found that two sets of critical parameters exist. First, there are minimum threshold values which must be exceeded to initiate the material destruction process. Second, critical values for the test parameters exist which should not be exceeded in order to ensure an effective cutting process. Based on statistical calculations it is found that the crack velocities of the materials have the most significant effect on the cutting process. The crack velocity of the material influences the depth of the cut, specific energy, and threshold parameters of the cutting process.

NOMENCLATURE

A,B	constants
b_w	cut width
C_{1-13}	constants
d_F	focussing nozzle diameter
d_M	average material grain size
E_{ab}^{dyn}	dynamic absorbed energy
E_M	target material Young's modulus
E_P	abrasive particle kinetic energy
E_{spec}	specific material removal energy
E_{thr}	critical destruction energy
h	depth of cut
h_0	maximum depth of cut
L	cut length
M	mass of disintegrated material
m_P	abrasive particle mass
$\dot{m}_P$	abrasive particle mass flow rate
N_m	machinability number
p	pump pressure
P_M	material property
p_{thr}	pump threshold pressure
r	coefficient of regression
t_{exp}	local exposure time
v	cutting head traverse rate
v_{cr}	target material crack velocity
V_M	volume of removed material
v_P	abrasive particle velocity
$v_{P,thr}$	abrasive particle threshold velocity
v_{thr}	critical cutting head traverse rate
v_W	target material P-wave velocity
z_a	sound impedance
χ	dynamic loading parameter
γ_M	target material fracture surface energy
ϵ	applied strain
ϵ_{cr}	ultimate strain
σ	applied stress
σ_c	target material ultimate compressive strength
σ_f	target material flow stress
$\dot{\sigma}$	stress rate
σ_t	target material tensile strength
ρ_a	abrasive material density
ρ_M	target material density

†WOMA Apparatebau GmbH, Postfach 141820, 47208 Duisburg, Germany. Feodor-Lynen-Scholar of the Alexander-von-Humboldt Foundation, Bonn, Germany, at the University of Kentucky, Center for Robotics and Manufacturing Systems, Lexington, KY, U.S.A.

‡University of Kentucky, Center for Robotics and Manufacturing Systems, Lexington, KY, U.S.A.

1. INTRODUCTION

The abrasive water jet (AWJ) is a new innovative tool for cutting rocks and rocklike materials. It can be used for cutting, pre-weakening and drilling of rocks, and for trenching heavily reinforced materials, e.g. steel reinforced concrete. Recent reviews on the capability of the abrasive water jet in the fields of mining and civil engineering are given in refs [1–3].

On the basis of jet generation, the abrasive water jet can generally be categorized as injection AWJ or suspension AWJ. For practical applications, injection AWJ is more commonly used. For this type of jet, the pump pressure ranges between $p = 100$ MPa and $p = 400$ MPa. An injection AWJ is formed by accelerating small abrasive particles (garnet, aluminum oxide, silica carbide) through contact with a high velocity plain water jet. This process is illustrated in Fig. 1. A typical abrasive grain diameter is $d_P = 400$ μm. The plain water jet is formed in an orifice above the abrasive cutting head. The abrasives enter the cutting head at a separate entry. The mixing between abrasive, water and air takes place in a mixing chamber, and the acceleration process occurs in an acceleration tube or abrasive waterjet nozzle. The abrasive particles leave this nozzle at velocities of several hundred meters per sec. A high number of abrasives (10^5 per sec) leads to a high frequency impingement on the materials being processed. The intensity and the efficiency of the cutting process depend on several process parameters, such as pump pressure, orifice diameter, traverse rate, standoff distance, abrasive mass flow rate, abrasive type and mixing chamber geometry. This study is performed by using an injection AWJ system.

The abrasive water jet is a streamlike tool, similar to laser and electron beams, which is characterized by an unsteady material removal process. The most pronounced characteristic of AWJ-generated surfaces is the presence of striation marks which transpire below a region of relatively smooth surface finish. It is widely accepted that the striations are a result of the formation of steps on the cutting front. The concept of step formation was introduced in the water jet cutting research by Mohaupt and Burns [4]. It is not clear yet what physical phenomenon may cause the formation of steps and striations in brittle multiphase materials.

Probably the most extensive study on rocks exposed to abrasive water jet cutting was carried out by Heßling [5]. He investigated the influence of several process parameters, e.g. pump pressure, nozzle diameter and traverse rate, as well as the influence of selected material parameters. He found some significant relations between the depth of cut and some material properties, e.g. tensile strength, Young's modulus and fracture toughness. However, the study contains little discussion or interpretation of the experimental results. Also, no attempt was made to find mathematical expressions of the parameter influences on the cutting process. Hashish [6] divided the abrasive water jet cutting process into two stages, "cutting wear" and "deformation wear". He suggested that the material resistance in the "cutting wear" process is characterized by the material hardness, whereas the "deformation wear" resistance is defined by Young's modulus. This theory is controversially discussed [7] and is questionable for the cases of brittle multiphase materials, e.g. rocks, concretes and minerals. In a more systematic study [8] it was found that the resistance of brittle materials can be characterized by their idealized strain energy,

$$h \propto \frac{2 \cdot E_M}{\sigma_t^2} \quad (1)$$

but, interestingly, this relation did not hold for rock materials such as marble and granite. This may be due to the more complex stress–strain behavior of brittle pre-cracked materials. Zeng *et al.* [9] introduced a so-called "machinability number", N_m, to describe the resistance of materials against abrasive water jet attack,

$$N_m = A \cdot \frac{d_M \cdot \sigma_f}{\gamma_M \cdot E_M} + \frac{B}{\sigma_f}. \quad (2)$$

Typical values for rocks and concretes are in the range of $N_m = 300$–600, whereas metals have values of about $N_m = 100$. The lower the value of N_m the higher the material resistance against abrasive water jet cutting. This parameter has to be estimated by reference experiments and therefore it may lead to a correct order of materials according to their abrasive water jet cutting resistance. Nevertheless, the machinability number fails in relation to some physical parameters, such as the average grain size of the target material and their fracture energy.

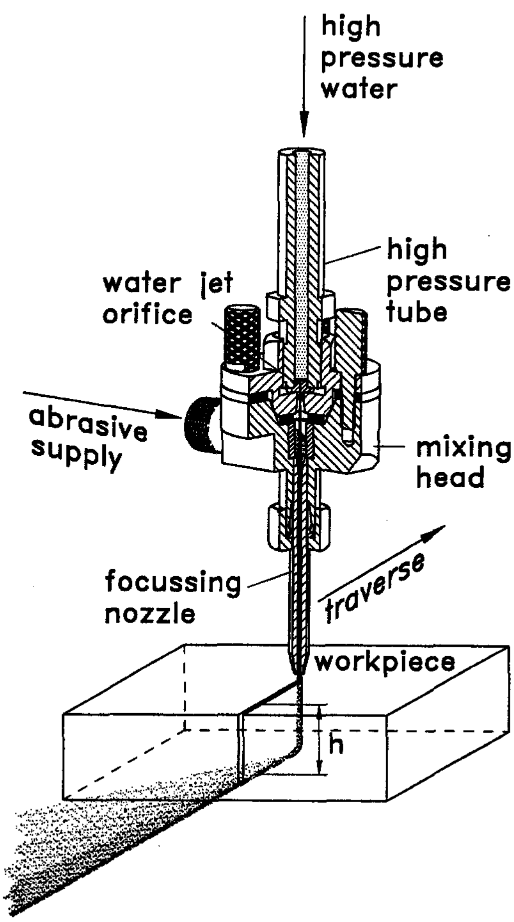

Fig. 1. Injection abrasive water jet cutting head and relevant test parameters.

2. OBJECTIVE AND GENERAL IDEA

The investigation is divided into two parts. The first part deals with the influence of the test parameters, i.e. the applied pump pressure, traverse rate and abrasive mass flow rate on the cutting process. From the practical point of view, these parameters are the most important in abrasive water jet cutting operations. The materials are cut with different parameter combinations and the depth of the generated cut is used to evaluate the parameter impact. Attempts are made to find mathematical equations to quantify the influence of these process parameters.

The second part contains an investigation into the influence of the target material properties on the cutting process. It is based on statistical methods. The relation between the depth of cut, h, as the most important

Table 1. Used types of regressions

Regression type	Regression equation $y = f(x)$
Linear	$a + b\cdot x$
Parabolic	$a\cdot x^b$
Polynomial	$a\cdot x^2 + b\cdot x + c$
Logarithmic	$a + b\cdot \ln x$

cutting result and the selected material properties, P_M, is defined as a function Φ,

$$\Phi = h(P_M). \tag{3}$$

Here, a specific material property can be substituted for P_M. To characterize the function Φ, four types of regressions were selected: linear regression, parabolic regression, polynomial regression and logarithmic regression. The formulas of these regressions are given in Table 1.

To evaluate a certain function Φ and the correlated material property P_M, respectively, the coefficient of regression, r, is used,

$$r = \frac{\sum_{i=1}^{n} (P_{M,i} - \bar{P}_M)^2 (h_i - \bar{h})^2}{\sqrt{\sum_{i=1}^{n} (P_{M,i} - \bar{P}_M)\cdot \sum_{i=1}^{n} (h_i - \bar{h})^2}}. \tag{4}$$

Here, h is the depth of cut which is selected as the most important target parameter in abrasive water jet cutting. In general, r is between 0 and 1, and the function with the highest r-value may be able to characterize the most significant material property.

3. EXPERIMENTAL SETUP AND PROCEDURE

3.1. Estimation of the material properties

For the investigation five different concrete mixtures were created and generated. The mechanical properties of these materials were influenced by changing the water–cement ratio, as well as the fineness of the used aggregate grains. After mixing and casting, these mixtures were cured and hardened for 28 days under water. After hardening the cylindrical specimens were tested (Fig. 2). The specimen dimensions were 30.8 cm in length and 15.24 cm in diameter. The compressive strength and Young's modulus of every mixture were estimated according to ASTM Standards C 39 and C 469. The results of these measurements are given in Table 2.

The stress–strain curves of the investigated materials were approximated by a parabolic function,

$$\sigma(\epsilon) = A\cdot(\epsilon - \epsilon_{cr}^2) + \sigma_C. \tag{5}$$

Here, σ_C is the ultimate compressive strength, and ϵ_{cr} is the corresponding strain. The integration of equation (3) between $\epsilon = 0$ and $\epsilon = \epsilon_{cr}$ yields the energy which is absorbed during the fracture of a certain volume of the material. Letting χ represent the dynamic loading during

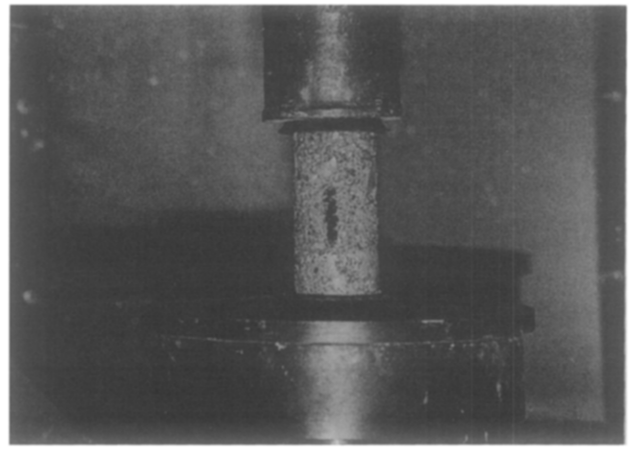

Fig. 2. Concrete specimens used for testing.

the abrasive water jet attack, which may influence the material behavior, the dynamic absorbed energy is [10],

$$E_{ab}^{dyn} = \chi(\dot{\sigma},\sigma_C)\cdot[0.\bar{3}\cdot A\cdot\epsilon_{cr}^3 + \epsilon_{cr}\cdot\sigma_C]. \tag{6}$$

The estimated values are given in Table 2. The crack velocities of the concrete samples are calculated based on [11]

$$v_{cr} = 0.25\cdot\sqrt{\frac{Y_M}{\rho_M}}. \tag{7}$$

3.2. Organization of the cutting experiments

The abrasive water jet cutting unit used for the cutting studies consists of an intensifier pump, abrasive cutting head, abrasive storage and metering system, catcher and CNC-controlled positioning system. The position of the cutting head is controlled using a x-y-z-positioning table.

After cutting, the dimensions of the generated cuts were measured, including depth of cut, cut width and cut length. The volume of the removed material was estimated by filling the kerfs with a fine grained (Mesh #36) material. A summary of 16 cutting experiments under different cutting conditions was carried out for each material (Fig. 3).

Regression analyses were carried out for each test parameter combination and each material property. Considering 16 parameter constellations, five material properties and four regression functions, requires 320 regression calculations. Consequently, 320 r-values were obtained to evaluate the influence of the material properties on the abrasive water jet cutting process.

The cutting conditions were changed by varying the test parameters pump pressure, traverse rate and abrasive

Table 2. Mechanical properties of the used materials

Material	Y_M (GPa)	σ_C (MPa)	E_{ab}^{dyn} (MJ/m³)	v_{cr} (m/sec)
#1	10.7	4.0	1.5	584
#2	24.1	12.5	7.9	845
#3	33.0	27.1	27.0	980
#4	34.3	34.2	40.9	975
#5	42.3	41.1	47.6	1062

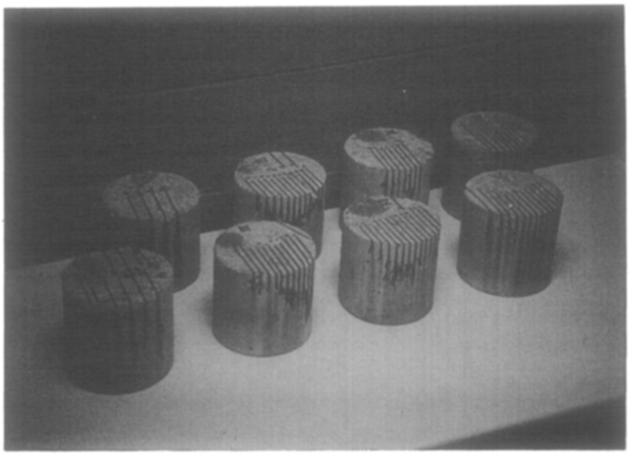

Fig. 3. Concrete specimen cut by abrasive water jet under different test conditions.

mass flow rate. The parameter ranges are listed in Table 3.

4. EXPERIMENTAL RESULTS AND REGRESSION ANALYSES

4.1. Results of the process parameter variations

The influence of the investigated test parameters, i.e. pump pressure, traverse rate and abrasive mass flow rate, on the depth of cut in the materials is illustrated in Fig. 4.

Figure 4(a) shows the relationship between the applied pump pressure and the depth of cut. Here, three interesting features can be noticed. First, the relation is non-linear with a decreasing progress at higher pump pressures, indicating that the material removal process is less efficient at higher pressure levels. In the first almost linear stage, the depth of cut increases rapidly due to the increasing kinetic energy of the impacting abrasive particles with increasing pump pressure.

$$E_P = \tfrac{1}{2}\cdot m_P\cdot v_P^2, \tag{8}$$

$$v_P \propto \sqrt{p}. \tag{8a}$$

If the pump pressure is increased further, losses due to a poorer mixing efficiency [12], abrasive particle fragmentation [13] and damping effects in the deeper kerfs [14] may reduce the progress of the material removal process. Second, a critical pump pressure, p_{thr}, can be noticed at the intersection of the pump pressure axis and the depth function which describes the minimum pressure required to cut the material. This pressure is usually known as the material "threshold pressure". It can be seen that this parameter increases with an increase in the material strength properties. The threshold pressure is discussed later in this paper. Finally, it can be seen that material #1 shows a comparatively low resistance against AWJ cutting, whereas the curves of materials #3– # 5 are close together. Mathematically, the relations in Fig. 4(a) can be described by,

$$h(p) = C_1\cdot(p - p_{thr})^{C_2}. \tag{9}$$

Here, $C_2 < 1$.

The influence of the traverse rate on the depth of cut is shown in Fig. 4(b). Again, three typical features can be noticed. As the measurement results illustrate, the cutting process is very sensitive to traverse rate changes in the range of small traverse rates. In this range, even small variations in the traverse rate yield significant changes in the depth of cut. For very low traverse rates it can be assumed that the cutting process has some similarities with a piercing process. In particular, damping processes due to an abrasive-water film on the bottom of the generated kerf [14] may play a significant role in determining the material removal process. Therefore, it is assumed that the depth of cut in a material has a constant value, $h = h_0$, for very low traverse rates. Finally, for very high traverse rates, the function may cross the v-axis at a critical traverse rate $v = v_{th}$. If this traverse rate is exceeded, almost no material removal will occur because the number of impacting abrasive particles becomes very small and the water may not be able to penetrate the material. These relations can be expressed by,

$$h(v) = h_0\cdot\left[\frac{-\ln v}{\ln v_{thr}} + 1\right]. \tag{10}$$

The critical traverse rate, v_{thr}, may be related to the crack velocity in the materials as shown in ref. [15] for plain water jet cutting of concrete. Figure 5 indeed shows a significant relation between the crack velocity of the materials and the threshold traverse rates estimated from equation (10).

The temporal development of the cutting process is alternatively illustrated in Fig. 4(c) where the depth of cut vs the local exposure time is plotted. The local exposure time is given by,

$$t_{exp} = \frac{d_F}{v}. \tag{11}$$

It can be assumed that the progress of the exposure time function significantly starts to drop at long exposure times, and that the function may approximate the maximum possible depth, h_0. Also, it can be seen that a threshold exposure time, t_{thr}, exists which has the same physical meaning as the threshold traverse rate in equation (10).

Figure 4(d) illustrates the influence of the abrasive mass flow rate on the cutting process. For low abrasive mass flow rates ($\dot{m}_P < 6$ g/sec) the depth of cut increases rapidly and almost linearly with an increase in the

Table 3. Cutting conditions and parameters

Test parameter	Symbol	Unit	Range
Pump pressure	p	MPa	100–350
Traverse rate	v	mm/sec	2.0–12.0
Abrasive mass flow rate	$\dot{m}_P$	g/sec	6.1–19.1
Abrasive size	—	mesh	# 36
Abrasive type	—	—	garnet

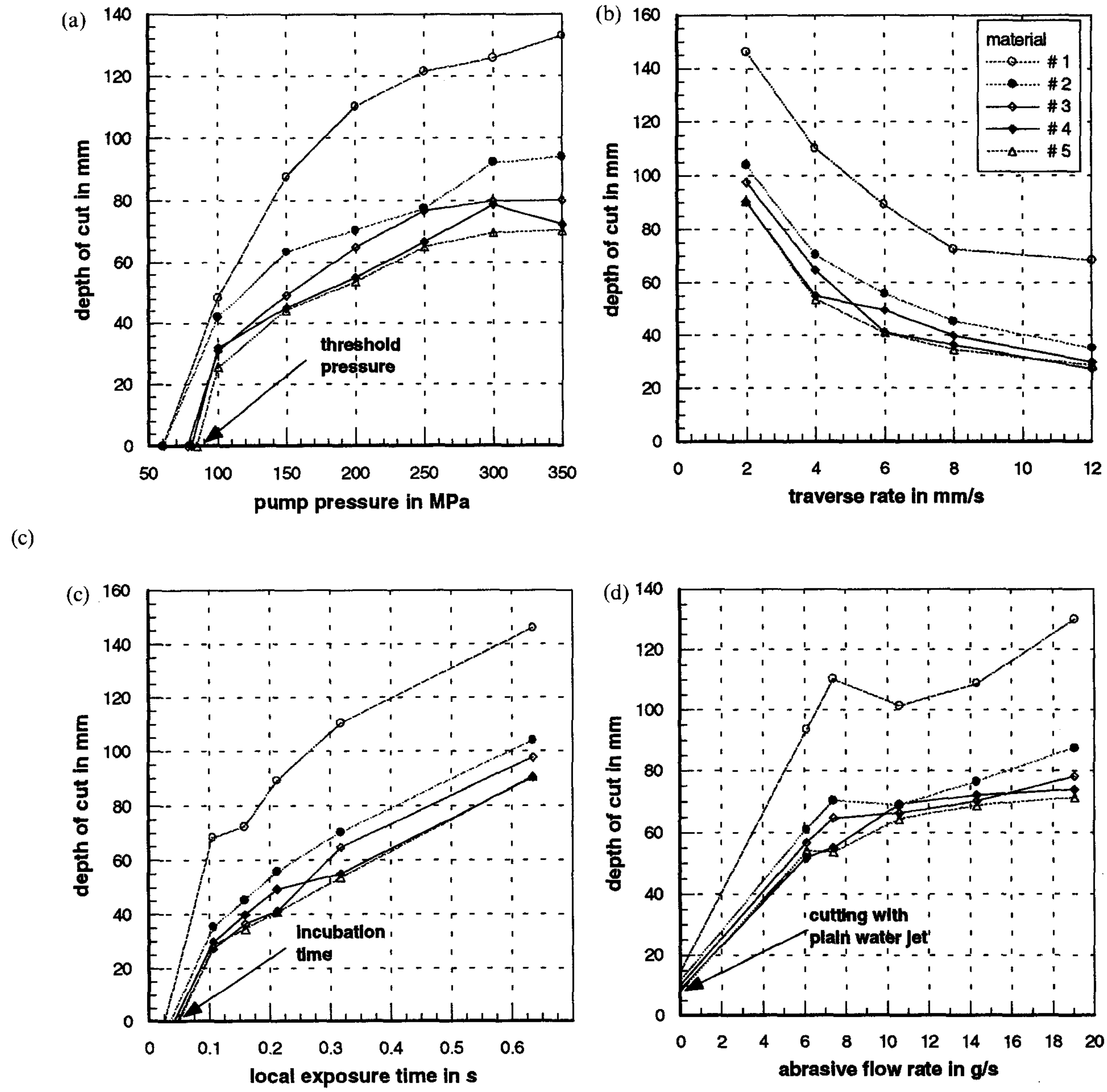

Fig. 4. Test parameters influence on the depth of cut in the investigated materials. (a) Pump pressure. (b) Traverse rate. (c) Local exposure time. (d) Abrasive mass flow rate.

abrasive mass flow rate. This may be due to the increased number of impacting abrasive particles which leads to an accelerated material removal process. Nevertheless, for the investigated abrasive mass flow rate range ($\dot{m}_P = 6.12$ g/sec to $\dot{m}_P = 19.05$ g/sec) the influence of the abrasive mass flow rate on the depth of cut is weak. The reason may be that for the given process condition, including mixing between the water jet and abrasive particles as well as cutting, a critical abrasive mass flow rate exists. Beyond this typical flow rate, the abrasive number is too large for efficient acceleration and cutting. This leads to a loss of efficiency in the mixing chamber as well as in the cut kerf due to friction, damping, particle collision and particle fragmentation. This assumption was recently experimentally supported by acoustic emission measurements on concrete samples subjected to abrasive water jets [16]. Therefore, a further increase in the abrasive mass flow rate will not significantly increase the depth of a cut. A possible mathematical description of the abrasive mass flow rate offers the equation,

$$h(\dot{m}_P) = h_0 \cdot [1 - e^{-C_3 \cdot \dot{m}_P}] \quad (12)$$

which covers all essential features of the curves plotted in Fig. 4(d), except that for $\dot{m}_P = 0$ it may be still possible to cut the material due to the high kinetic energy of the plain water jet.

4.2. *Results of the material property variations*

The results of the investigations on the influence of the material properties on the abrasive water jet cutting process are summarized in Fig. 6. The relation between the dynamic absorbed energy as given by equation (6) and the depth of cut is shown in Fig. 6(a). As Table 4 shows, this relation can be fitted very reasonably by a parabolic regression

$$h(E_{ab}^{dyn}) = C_4 \cdot (E_{ab}^{dyn})^{C_5}. \quad (13)$$

This relation confirms results which are obtained by using a simplified abrasive water jet process model in ref. [10]. In fact, in a logarithmic expression, equation (13) would fit the results of Matsui *et al.* [8] very well. Therefore, the bad correlation for rocks in ref. [8] can be overcome by using the real stress–strain curve of these materials and replacing the right part of equation (1) by equation (6). The relation between Young's modulus and the depth of cut in the samples is shown in Fig. 6(b). It is found that this relation can be characterized by a negative second order polynomial,

$$h(Y_M) = C_6 \cdot Y_M^2 + C_7 \cdot Y_M + C_8 \tag{14}$$

which confirms at least equations (1) and (2) which suggest a reduced abrasive water jet cutting performance with an increase in Young's modulus. Figure 6(c) illustrates the influence of the compressive strength on the depth of cut. As shown in Table 4 the results can be fitted reasonably by a parabolic regression

$$h(\sigma_C) = C_9 \cdot \sigma_C^{C_{10}}. \tag{15}$$

The relation between the crack velocity and the estimated depths of cut which is shown in Fig. 6(d) can effectively be approximated by a second order polynomial (Table 4),

$$h(v_{cr}) = C_{11} \cdot v_{cr}^2 + C_{12} \cdot v_{cr} + C_{13}. \tag{16}$$

The calculations of the regression coefficients are summarized in Table 4. The table shows the relation between the investigated material properties and the regression coefficients estimated according to equation (4). The single regression coefficient characterizes the coefficient of the regression functions given in equations (13)–(16), whereas the average regression coefficient, $\bar{r}$, has to be considered as the average value from all regressions carried out.

The results from this part of the study indicate that the material property parameter crack velocity shows the strongest relation to the kerfing process with an average correlation coefficient of $\bar{r} = 0.978$. This material property may be able to describe the behavior of the concrete materials under the given loading with the highest accuracy. It is followed by Young's modulus, compressive strength, and absorbed energy.

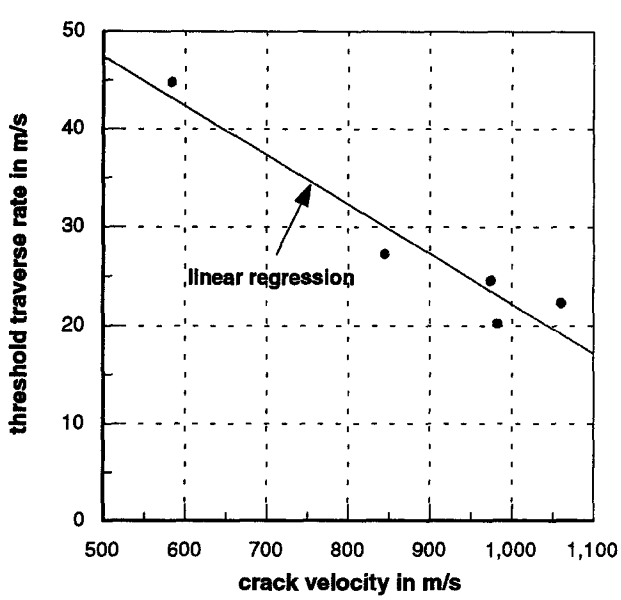

Fig. 5. Relation between crack velocity and minimum threshold traverse rate.

5. DISCUSSION

The investigations have shown that the crack velocity of the materials may be able to describe their resistance against abrasive water jet cutting. This aspect is not covered by any of the existing abrasive water jet cutting models. The crack velocity can be related to the wave velocity of the materials. As shown in ref. [11] the P-wave velocity (v_W) of concretes characterizes their maximum possible theoretical crack velocity and is related to the crack velocity by

$$v_W \cong 4 \cdot v_{cr}. \tag{17}$$

Using this relation, the measurements confirm results from Heßling [5] who found a good relation between the wave velocity and depth of cut in rocks cut by abrasive water jets. A linear correlation between the specific energy in plain water jet rock cutting and the P-wave velocities of rocks was observed in ref. [17] which may be discussed later. In the work by Evans *et al.* [18,19] on ceramics, which may be comparable to the concrete because of their quasi-brittle behavior, it was shown experimentally that a critical threshold velocity of impacting particles must be overcome to introduce damage due to fracture. The relation between this threshold parameter and the P-wave velocity is [19],

$$v_{P,thr} \geqslant C \cdot \frac{1 + \dfrac{v_W \cdot \rho_M}{z_a}}{\rho_a \cdot \dfrac{v_W \cdot \rho_M}{z_a}}. \tag{18}$$

This equation has to be solved by iterative methods. A simplification of this equation is given in ref. [18],

$$v_{P,thr} = \text{const}_1 \cdot v_W^{0.33}. \tag{19}$$

The velocity of the solid particles used in an abrasive water jet, v_P, can be expressed by the pump pressure, p. The relation between both parameters is given by equation (8a). The threshold particle velocity, $v_{P,thr}$, in equation (19) can then be substituted by the threshold pump pressure, p_{thr}. The threshold pressure can simply be estimated experimentally by plotting the applied pump pressure against the depth of cut [Fig. 4(a)]. Figure 7 shows the influence of the materials crack velocities on their threshold pressures as estimated in this study. The results can be fitted very well with equation (19) if v_W is replaced by equation (17).

A significant relation between the wave velocity and the comminution rate of brittle materials was observed in ref. [20]. Based on assumptions about the physics of material strength, Dahlhoff [21] developed a relation

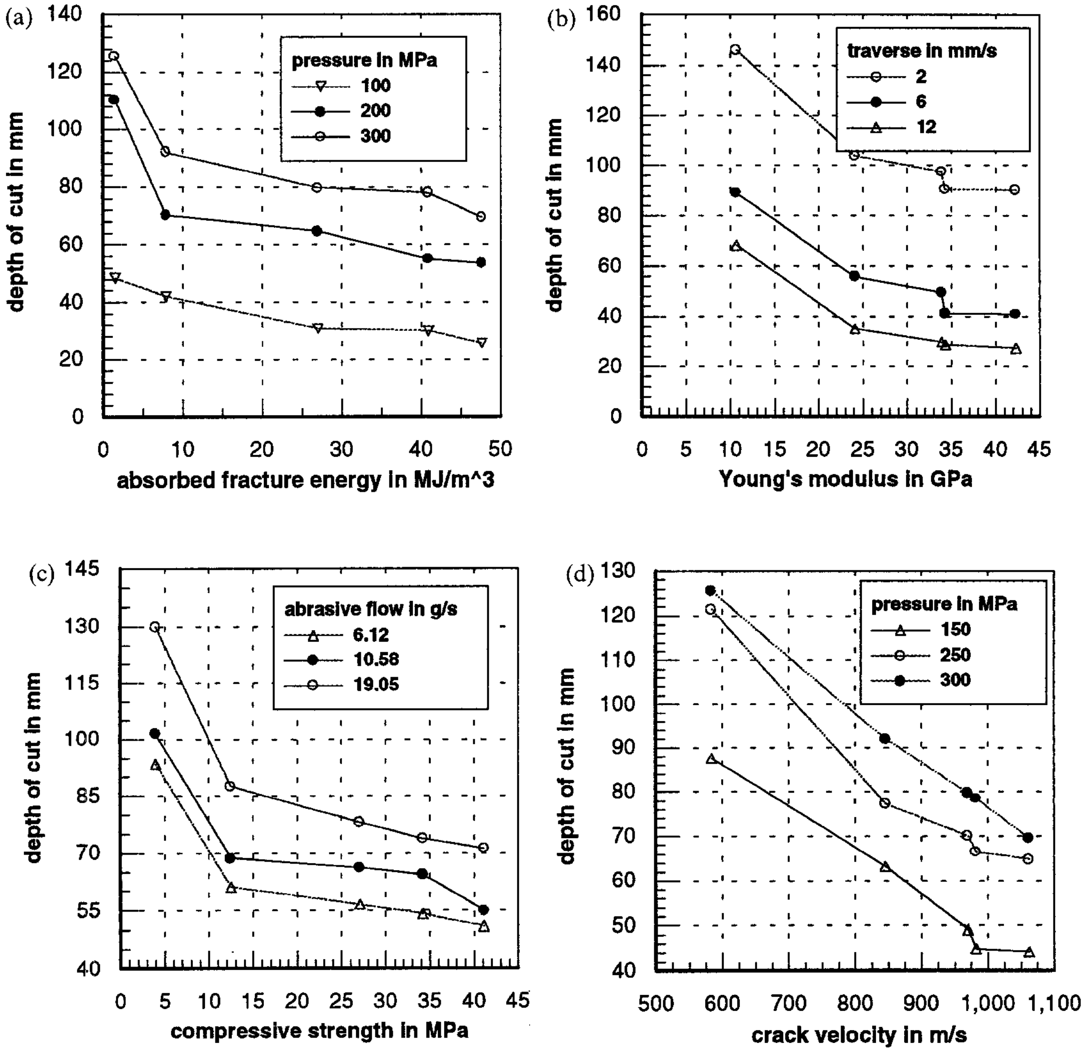

Fig. 6. Material parameters influence on the depth of cut. (a) Absorbed energy. (b) Young's modulus. (c) Compressive strength. (d) Crack velocity.

between the critical energy for material destruction and the wave velocity,

$$E_{\mathrm{thr}} = \mathrm{const}\cdot M\cdot v_{\mathrm{W}}^{2}. \tag{20}$$

Here, M is the mass of the disintegrated material. Writing $M = V_{\mathrm{M}}\rho_{\mathrm{M}}$, and rearranging equation (20) yields

$$\frac{E_{\mathrm{thr}}}{V_{\mathrm{M}}} = E_{\mathrm{spec}} = \mathrm{const}\cdot\rho_{\mathrm{M}}\cdot v_{\mathrm{W}}^{2}. \tag{21}$$

This equation implies a relation between the absorbed energy during the destruction of a certain material volume and the square of the wave velocity (crack velocity, respectively). This result does not confirm experimental results in ref. [17] where a linear relation between the specific kerfing energy of rocks cut by plain water jets and the wave velocity was found, but, as pointed out in ref. [17], the measurements were not accurately defined at high specific energy levels. Considering this fact, a quadratic relation may not be impossible. For the materials investigated in this study, a second order polynomial can be applied successfully to relate the crack velocity to the specific material removal energy confirming equation (21). A typical example is shown in Fig. 8.

For a constant abrasive water jet energy which may be realized by a constant pump pressure level and assuming $V_{\mathrm{M}} = h\cdot L\cdot b_{\mathrm{W}}$, equation (21) can be rewritten,

$$h = \mathrm{const}_4\cdot\frac{E_{\mathrm{spec}}\cdot\rho_{\mathrm{M}}}{b_{\mathrm{W}}\cdot L\cdot v_{\mathrm{cr}}^{2}} = \mathrm{const}\cdot v_{\mathrm{cr}}^{-2}. \tag{22}$$

This solution is identical with a parabolic regression for the crack velocity (Table 1) with the regression

Table 4. Results of the regression coefficient calculations

Regression → Parameter ↓	Linear	Parabola	Polynomial	Logarithm	$\bar{r}$
Absorbed energy	0.876	**0.976**	0.931	0.974	0.939
Young's modulus	0.962	0.975	**0.991**	0.981	0.977
Compressive strength	0.915	**0.978**	0.966	0.977	0.959
Crack velocity	0.977	0.968	**0.990**	0.978	**0.978**

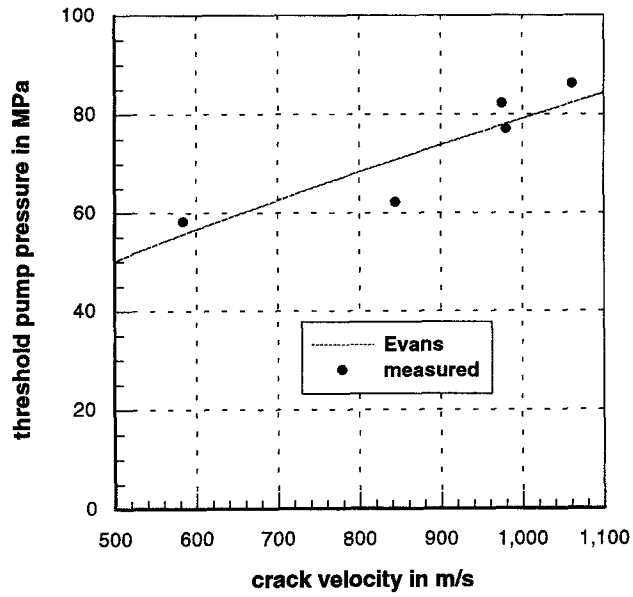

Fig. 7. Relation between crack velocity and threshold pump pressure.

parameters $a = \text{const}$ and $b = -2$. The fact that the polynomial regression, not this parabolic regression, has the highest regression coefficient in this study, can be explained by the restriction that $V_M = h \cdot L \cdot b_W$, and so equation (22) is valid for shallow kerfs and certain abrasive mass flow rates only. In contrast, the polynomial regression considers all depths of cut and the entire test parameter range.

6. SUMMARY AND CONCLUSIONS

A systematic study was carried out to investigate the behavior of artificial rocks against the action of abrasive water jets. The influence of the test parameters, such as pump pressure, traverse rate and abrasive mass flow rate was investigated. The materials are very sensitive to changes in these parameters at low pump pressures, low traverse rates and low abrasive mass flow rates. A critical threshold pump pressure, as well as a critical threshold traverse rate exist which must be exceeded to introduce an effective cutting process. Generally, each material seems to be characterized by a maximum "saturation depth of cut" which will be achieved at very high pump pressures, low traverse rates and high abrasive mass flow rates. The influence of the investigated test parameters on the depth of cut is generally non-linear.

The influences of the compressive strength, Young's modulus, absorbed energy and crack velocity were investigated based on regression coefficient calculations. It was found that the crack velocities of the materials are usable parameters to describe the "cutting resistance" against abrasive water jet cutting. The relation between the crack velocity and depth of cut can be characterized by a second order polynomial ($r = 0.99$) for a wide range of cutting conditions. Additionally, it seems that the crack velocity is useful for describing the critical threshold pump pressure and the specific energy of abrasive water jet cutting processes in rocklike materials.

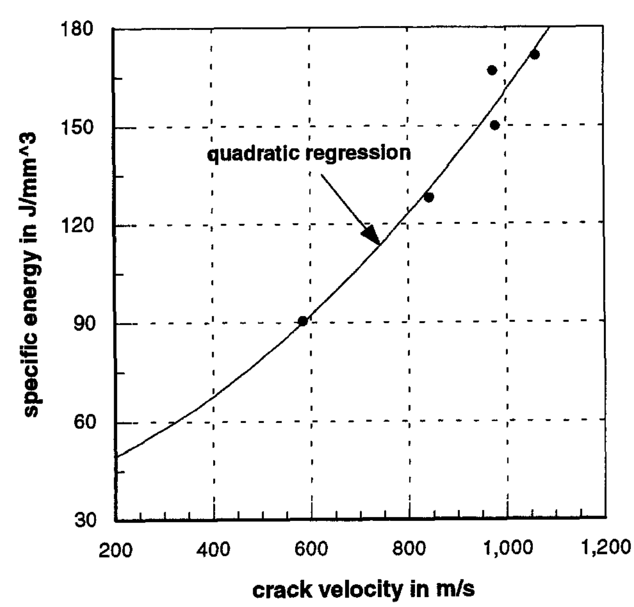

Fig. 8. Relation between crack velocity and specific material removal energy.

Acknowledgements—The authors are thankful to the Center for Robotics and Manufacturing Systems, University of Kentucky, Lexington, KY, and to the Alexander von Humboldt-Foundation, Bonn, Germany, for financial support. Thanks are addressed to the Kentucky Transportation Center for preparing and testing the specimens and to Mr I. Eusch for conducting part of the experiments.

Accepted for publication 30 July 1996.

REFERENCES

1. Vijay M. and Wenzhou Y. Water jet cutting techniques for processing of hard rock material. *Int. J. Surf. Min.* **3**, 59–69 (1989).
2. Momber A. *Handbuch Druckwasserstrahl-Technik*. First Edition, Beton GmbH, Düsseldorf (1993).
3. Momber A. Water jet usage in civicl engineering. *Geomechanics 93* (Edited by Rakowski Z.), pp. 367–378. A. A. Balkema, Rotterdam (1994).
4. Mohaupt U. H. and Burns D. Machining unreinforced polymers with high velocity water jets. *Exper. Mech.* **14**, 152–157 (1974).
5. Heßling M. Grundlagenuntersuchungen über das Schneiden von Gestein mit abrasiven Höchstdruckwasserstrahlen. Ph.D. thesis, RWTH Aachen (1988).
6. Hashish M. Wear modes in abrasive water jet machining. *PED* **54**, 141–153 (1991).
7. Arola D. and Ramulu M. Mechanisms of material removal in abrasive waterjet machining of common aerospace materials. *7th American Water Jet Conference*, Seattle, U.S.A., pp. 43–64 (1993).
8. Matsui S. *et al.* Prediction equations for depth of cut made by abrasive water jet. *6th American Water Jet Conference*, Houston, U.S.A., pp. 31–41 (1991).
9. Zeng J., Kim J. and Wallace R. J. Quantitative evaluation of machinability in abrasive waterjet machining. *PED* **58**, 169–179 (1992).
10. Momber A. and Kovacevic R. The influence of the stress–strain behaviour of quasi-brittle materials on their machinability by abrasive water jets. In preparation.
11. Curbach M. and Eibl J. Crack velocity in concrete. *Engng Fracture Mech.* **35**, 321–326 (1988).
12. Momber A. and Kovacevic R. Energy dissipative processes in high speed water-solid particle erosion. *Proc. ASME Heat Transfer and Fluids Engineering Division*, New York, U.S.A., pp. 243–256 (1995).
13. Simpson M. Abrasive particle study in high pressure water jet cutting. *Int. J. Water Jet Tech.* **1**, 17–28 (1991).
14. Yong Z. and Kovacevic R. Simulation of effects of water-mixture film on impact contact in abrasive waterjet machining. *Int. J. Mech. Sci.*, accepted for publication (1996).

15. Momber A. and Kovacevic R. Fundamental investigations on concrete water by high velocity water flow. *Wear* **177,** 55–62 (1994).
16. Momber A., Mohan M. and Kovacevic R. Acoustic emission measurements on brittle materials during abrasive waterjet cutting. *First Int. Machining and Grinding Conference*, Dearburn, U.S.A., pp. 439–458 (1995).
17. Agus M. *et al.* The influence of rock properties on water jet performance. *7th American Water Jet Conference*, Seattle, U.S.A., pp. 427–442 (1993).
18. Evans A. G. Impact damage in ceramics. *Fract. Mech. of Ceramics* (Edited by Brandt R. C. *et al.*), pp. 303–321. Plenum Press, New York (1978).
19. Evans A. G., Gulden M. E. and Rosenblatt M. Impact damage in brittle materials in the elastic plastic response regime. *Proc. Roy Soc. Lond.* **A361,** 343–365 (1978).
20. Kiesskalt S. and Dahlhoff S. Praktische Bedeutung zweier zerkleinerungsphysikalischer Effekte. *Chemie-Ing. Techn.* **37,** 277–283 (1965).
21. Dahlhoff B. Zusammenhang zwischen der Zerkleinerungsgeschwindigkeit und Schall-Geschwindigkleit in spröden Feststoffen. *Chemie-Ing. Techn.* **67,** 1112–1116 (1967).